

The effects of enhancing the crosslinking degree in high internal phase emulsion templated poly(dicyclopentadiene) cured by Ring-opening Metathesis Polymerization by a crosslinking comonomer.

*Efthymia Vakalopoulou and Christian Slugovc**

E. Vakalopoulou, Prof. C. Slugovc
Institute for Chemistry and Technology of Materials, Graz University of Technology,
Stremayrgasse 9, A 8010 Graz, Austria
E-mail: slugovc@tugraz.at

The effect of enhancing the crosslinking degree in polyHIPEs made from dicyclopentadiene by additionally using a crosslinking comonomer is described. Foams of 80 % porosity with 10-40 w% comonomer content in the continuous phase are prepared and show similar porosities and morphological characteristics as foams prepared with dicyclopentadiene alone. Assessing the mechanical properties reveals that the ductility is decreasing while the stiffness of the samples is increasing with increasing comonomer content. The foams containing the crosslinking comonomer take up at least their five-fold mass of toluene thereby swelling to at least 30 v%. Upon drying of the swollen specimens, their initial shape and porosity are recovered. This feature distinguishes them from polyHIPEs made from dicyclopentadiene only.



1. Introduction

The curing of high internal phase emulsions (HIPE) featuring monomers in its continuous phase is an important and popular way to prepare macroporous polymer foams. ^[1,2] Such porous materials are often named polymerized HIPEs, abbreviated as poly(HIPE)s. Typically, materials with open-porous highly interconnected architectures are obtained, which find applications in many different fields. ^[1,2] Very recent examples of their use in separation, ^[3,4,5,6] flow-through techniques, ^[7] biotechnology, ^[8] drug release, ^[9,10] energy storage, ^[11] sensing ^[12] or food preservation ^[13,14] illustrate their versatility. polyHIPEs are prepared by many polymerization techniques but above all (free) radical polymerization of styrenes and electron deficient olefins is used. ^[1] One of the more exotic polymerization techniques for curing HIPEs, first introduced by Deleuze et al. ^[15,16] is Ring-opening Metathesis Polymerization (ROMP). ROMP became an important technique, because it enables the preparation of polyHIPEs from dicyclopentadiene (**DCPD**) as the monomer and the according foams exhibit unique and favorable mechanical properties usually not associated with this class of porous materials. **pDCPD** based foams are characterized through high strength combined with high toughness. ^[17,18,19,20] In other words, the porous materials are stiff and ductile at the same time (the Young's modulus of a foam with 80% porosity is about 116 MPa, the modulus of toughness is around 600 kJ/m³). ^[21] Moreover, the high unsaturation of the polymer scaffold allows for a huge variety of chemistries for further functionalizing **pDCPD** foams. ^[17,22,23,24,25,26] The combination of these two features led to the use of emulsion templated **pDCPD** foams as separators in Li-ion batteries, ^[27] as templates for making porous oxides, ^[28,29] for making composite materials ^[28,29,30,31,32,33] and carbon foams, ^[34] for stabilization of enzymes ^[35] or for detoxification of nerve gases. ^[24,25] The most important drawback of **pDCPD** based polyHIPEs is their relatively fast oxidation in air, ^[17,24,25] but also the change of the macroscopic shape and porous structure upon drying off of nonpolar solvents is unfavorable. ^[36] In fact, a shape

recovery upon drying is worthwhile for all applications which demand a switching between dry and swollen state and for making an a posteriori chemical functionalization of the foams possible.

Herein we report **pDCPD** based macroporous foams which can be swollen in nonpolar solvents and recover their original shape upon drying. The approach towards the new foams is shown in Figure 1. By using an easily accessible crosslinking comonomer (**CLC**) bearing two norbornene moieties in addition to **DCPD**, the crosslinking degree of the polymer phase is increased and this effect is held responsible for the structure recovery upon drying of swollen monolithic foam specimens. As a side effect, it can be anticipated that free norbornenes further facilitate a post-polymerization functionalization of the foams by e.g. inverse electron demand Diels Alder^[23,37,38] or thiol-ene chemistries.^[39,40]

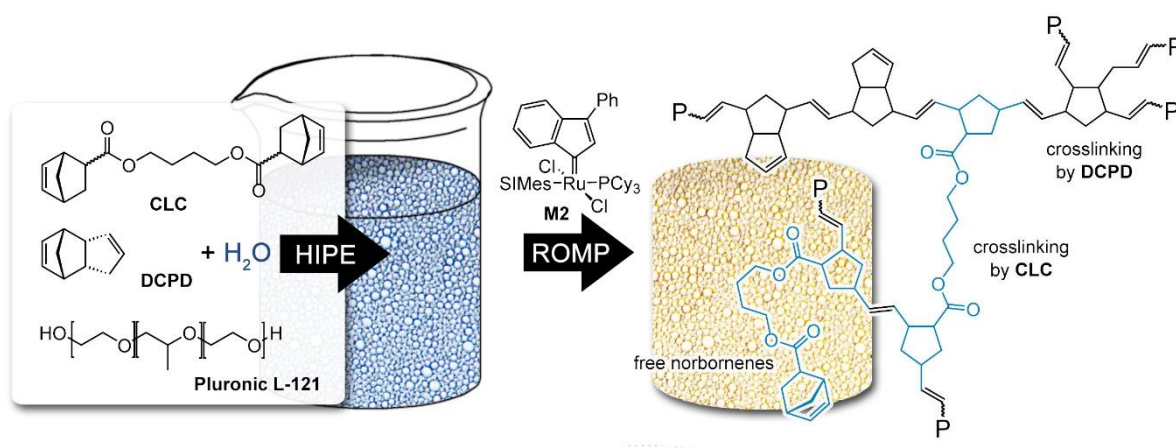


Figure 1. Formulation and process to prepare the foams of this study.

2. Results and Discussion

2.1. Preparation

The crosslinking comonomer (**CLC**) was prepared by adding a slight excess of freshly distilled cyclopentadiene to neat butane-1,4-diyl diacrylate under cooling and stirring. Upon

determining full conversion of the acrylate-groups surplus cyclopentadiene was evaporated under vacuum. Dicyclopentadiene formed as the only byproduct and was removed by flash chromatography. This purification step was done to properly characterize the **CLC**, however it could be left out in practice because **CLC** and **DCPD** are the two monomers employed in the following. Foams of 80% nominal porosity were prepared with a mixture of **DCPD** and a varying share of **CLC** (10-40 wt% in the mixture with **DCPD**) as the monomers. Pluronic L-121 (7 wt% in respect to the monomer mixture) served as the surfactant for stabilizing the HIPE obtained upon addition of water (40 mL) to the mixture of the monomers and the surfactant under stirring (Figure 1). The initiator **M2**^[41] (1:15000 in respect to the molar amount of norbornene moieties; dissolved in toluene) was used to cure the HIPEs at 80°C for 3 h in closed molds. The resulting polyHIPE specimens were demolded, submersed in acetone and kept there for 15 min. Subsequent drying gave white monolithic macroporous foams. As a reference, samples prepared by using only **DCPD** as the monomer were prepared similarly. HIPEs containing 50 w% **CLC** or more showed fast phase separation and were not investigated herein.

2.2. Morphology

Upon curing the specimens exhibited a volume shrinkage of about 2% and featured apparent densities in the range from 0.20 to 0.23 g·mm⁻³. The skeleton density is about 1.09 g·mm⁻³ and is gradually increasing from **P0** to **P40**. The foams exhibited a porosity close to the nominal porosity of 80%. Measured porosities were in between 79% and 83% depending on the method for determining them (Table 1 and vide infra for a discussion). Accordingly, increasing the amount of **CLC** from 0 to 40 w% in the formulation did not cause significant changes of densities and porosities of the resulting specimens. In contrast, slight differences in the morphology of the interior of the monoliths could be noted. All specimens exhibited the typical throughout open polyHIPE morphology characterized by the presence of voids, which are

Table 1. Apparent density, volume shrinkage, porosity and skeleton density of the foams **P0-P40**.

Sample	Apparent Density ^{a)} [g/cm ⁻³]	Volume shrinkage ^{b)} [%]a	Porosity (mass loss) ^{c)} [%]	Porosity (EtOH) ^{d)} [%]	Skeleton density ^{e)} [g/cm ⁻³]
P0	0.2023±0.0022	2.1±0.7	80.4±0.3	81.7±1.0	1.08±0.1
P10	0.2034±0.0018	2.7±1.0	79.2±0.4	82.8±0.6	1.08±0.1
P20	0.2165±0.0038	2.6±0.6	79.1±0.6	82.7±0.3	1.09±0.1
P30	0.2344±0.0083	2.2±0.5	79.4±0.1	83.2±0.6	1.10±0.1
P40	0.2203±0.0042	1.6±1.2	78.9±0.7	82.8±0.5	1.10±0.1

^{a)} retrieved from dividing the mass of the specimens by their volume; ^{b)} percentage of the specimens volume compared to the molds volume; ^{c)} calculated from the mass loss during polymerization taking the volume change in consideration; ^{d)} calculated from mass increase by immersion of EtOH taking the volume change into consideration; ^{e)} calculated from mass and assuming 80% porosity

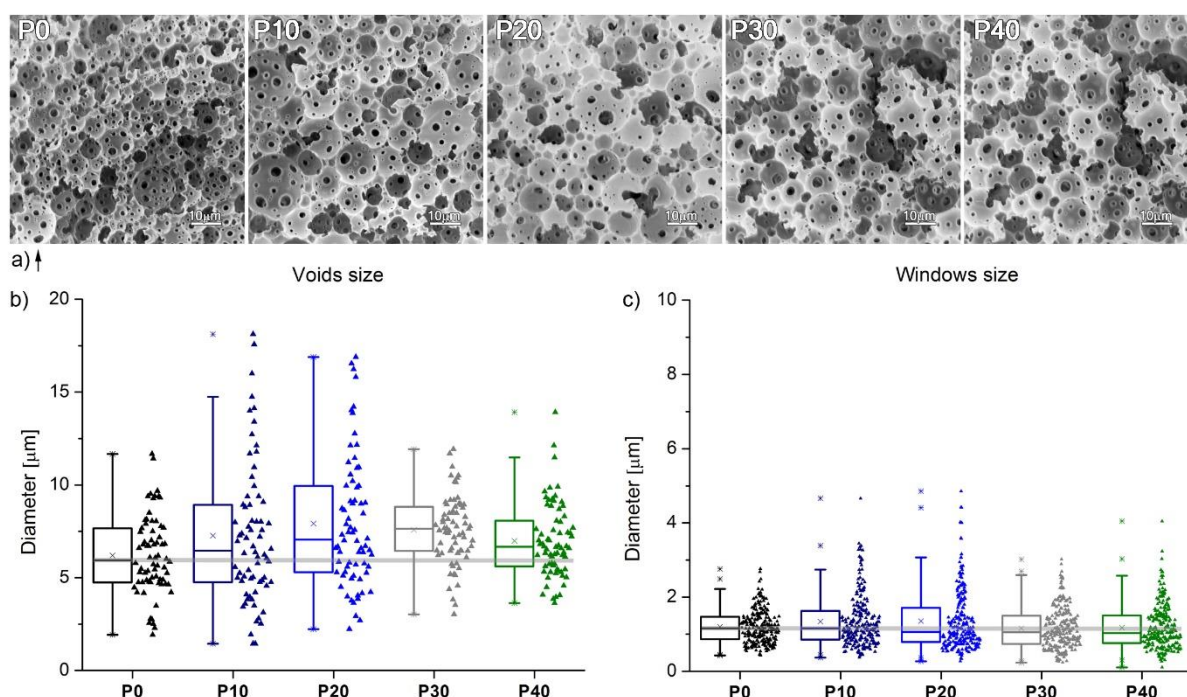


Figure 2. a) scanning electron micrographs of the (oxidized) foams **P0-P40**; box-whisker/bee swarm plot of b) void and c) window size distributions (median: horizontal line in the box; quartiles: upper and lower limit of the box, the boxes represent a restricted area where half of the overall values are included; whiskers: 1.5·IQR). The grey bars visualize the median voids and windows diameter for **P0**.

interconnected with windows. Voids and windows sizes were assessed from SEM measurements of broken samples and results are gathered in Figure 2. Compared to the

reference sample **P0** ($5.95 \pm 2.05 \mu\text{m}$) all median voids diameter of **P10-P40** are larger (in the range of $6.67 \pm 3.55 - 7.95 \pm 3.39$). The distribution of the diameters becomes distinctly larger when going from **P0** to **P10** and **P20** and becomes even smaller in **P30** and **P40** (Figure 2b). Windows diameter and their distribution stay similar with values from 1.16 ± 0.42 to $1.36 \pm 0.81 \mu\text{m}$ over the whole series (Figure 2c).

2.3. Investigation of the chemical composition

Infrared spectroscopy revealed the presence of **CLC** and the surfactant in the polymeric skeleton of the foam (Figure 3). The C=O stretching vibration of the ester's carbonyl group was detected at 1727 cm^{-1} and is gradually decreasing with decreasing **CLC** loading from **P40** to **P10**. A very small absorption at this wavelength was also detected in **P0** and is ascribed to minor oxidation of **pDCPD**.^[17] The C-O stretching vibration of the C-O bonds in **CLC** was observed at 1169 cm^{-1} just next to the C-O stretching vibration of the ether groups in Pluronic L121 (1105 cm^{-1}). Accordingly, IR revealed that the surfactant was not completely removed from the samples during the extraction step. Comparing IR spectra of a **P40** sample before and after extraction makes clear that the surfactant content is reduced by this step. Although all samples were treated in the same way, the amount of Pluronic L121 is different in all samples being highest in **P20**. It is plausible to assume that increasing the **CLC** share is facilitating the accommodation of Pluronic L121 in the nonpolar phase. However, the decrease of Pluronic L121 content at higher **CLC** loadings cannot be explained. The polymer backbone is characterized by C-H bending vibrations of double bonds from *trans*-connected repeating units (973 cm^{-1}) and *cis*-connected repeating units as well as from cyclic olefins (755 , 732 and 706 cm^{-1}). Vibrations from either ring-opened or not ring-opened **CLC** and **pDCPD** superimpose in a way that a quantification of crosslinking from these data is not possible.

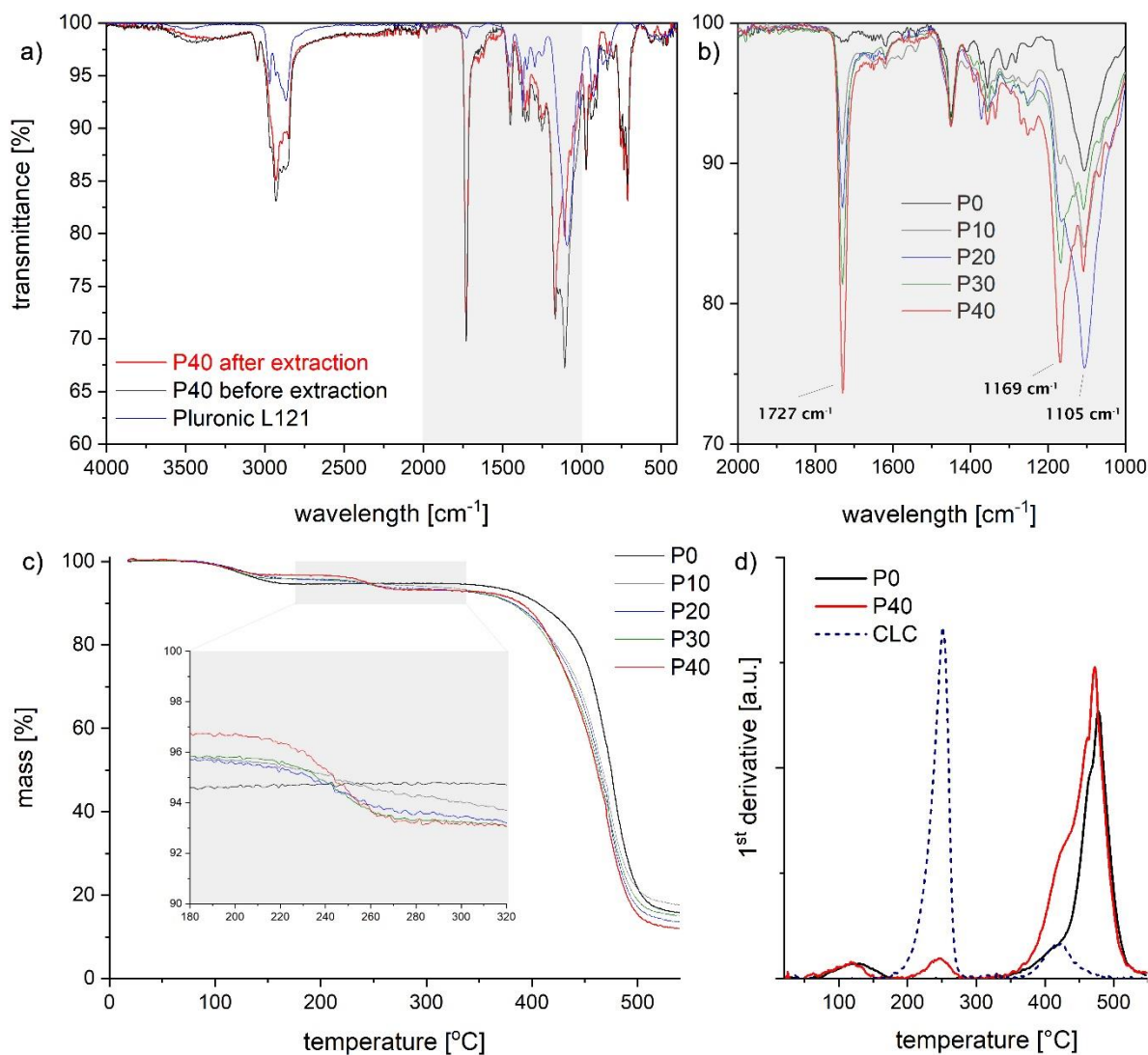


Figure 3. a) IR spectra of **P40** after and before extraction and of Pluronic L121; b) detail of the IR spectra of **P0-P40**; c) TGA curves of **P0-P40** showing in the inset a magnification of the mass loss due to the retro Diels-Alder reaction of free norbornene groups from **CLC**; d) first derivative of the TGA results for **P0**, **P40** and the monomeric **CLC**.

Thermal gravimetric analysis (TGA) allows quantifying residual (not polymerized) norbornene ester moieties of **CLC**. A mass loss characterized by an inflection point at around 240 $^{\circ}\text{C}$ is attributed to the retro-Diels Alder reaction of norbornene ester moieties of **CLC**. As evident from TGA of the **CLC** monomer at that temperature, cyclopentadiene and the corresponding acrylate is formed (Figure 3d and Figure S5-S6). Both are volatile at 240 $^{\circ}\text{C}$ and evaporate while a smaller share thermally polymerizes forming presumably a polyacrylate (which composes at slightly lower temperatures than then ROMP derived polymer). With this knowledge, the mass

loss in **P10-P40** can be attributed to the evaporation of cyclopentadiene and the ratio of polymerized to unpolymerized norbornene moieties of **CLC** can be quantified. Data reveal that approx. in half of the **CLC** molecules one norbornene is not ring-opened. Assuming that every doubly ring-opened **CLC** is a junction point, a maximal crosslinking degree originating from **CLC** can be calculated. Values amount to 1.7, 4.1, 7.6 and 10.8 mol% junction points in **P10**, **P20**, **P30** and **P40**, respectively. In other words, the average chain in between a junction point bears about 60 repeating units in **P10** and about 10 in **P40**. The overall crosslinking degree, which should also take a ring opening of **DCPD**'s cyclopentene ring into account, could not be assessed. Further information gained from TGA comprise a minor mass loss of 3 ± 1.5 w% starting at 85°C. The inclination point was found at 123 ± 5 °C. This mass loss is most probably due to evaporation of toluene, which cannot be fully removed upon the drying procedure employed. Some evidence for this hypothesis comes from TGA investigations of bulk samples, i.e. non porous variants of the porous samples discussed here, which do not exhibit similar mass losses (Figure S6). Beside the discussed retro-Diels Alder reaction, the thermal stabilities of **P10-P40** are slightly lower than that of **P0**, which shows thermal degradation at temperatures above 350°C.

2.4. Swelling and Deswelling

The uptake capability of the foams **P0-P40** of different solvents was assessed by determining the weight and volume of disc-shaped specimens in wet state. Water, ethanol, *n*-pentanol, acetone and toluene were tested. Results are gathered in Figure 4a and b. Polar protic and polar aprotic solvents are accommodated mainly in the voids because no or low swelling of the specimens was detected. The water uptake (334 w%) is somewhat lower than the calculated value (387-399 w%) taking the range of the determined porosity of 79-83% into account. This observation might be best explained by the high surface tension of water, which does not permit

water to enter smaller structures. On the other hand, intrusion of water is nevertheless possible pointing to the presence of a polar surface of the foams likely formed by residual surfactant residing at the polymer's surface. Data retrieved for ethanol were used to determine the porosity (Table 1) albeit swelling was a little bit more pronounced than in the case of water. Less polar *n*-pentanol and acetone cause slightly more swelling than ethanol. The swelling increases when going from **P0-P40** probably because of the increasing amount of **CLC**

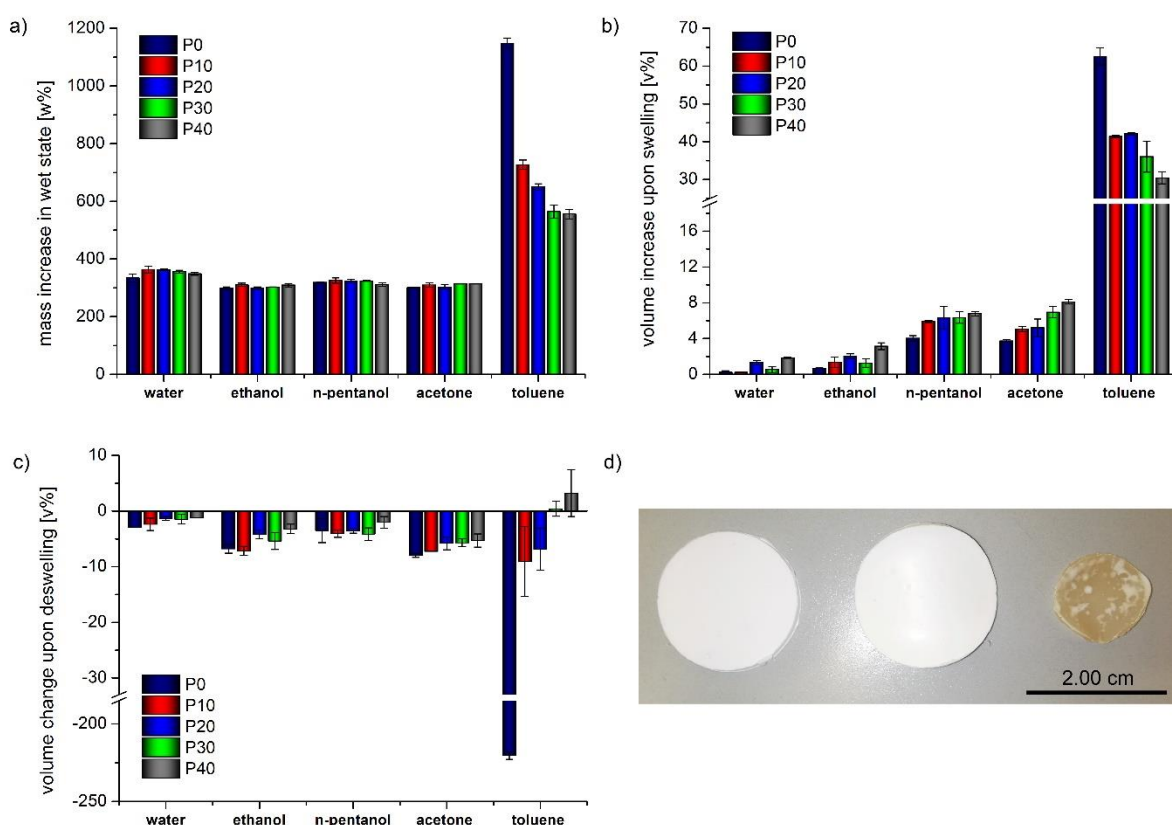


Figure 4. a) mass increase upon immersion of solvents; b) swelling of the samples; volume change upon drying the swollen samples expressed as v% in respect to the volume before swelling; d) photographs of a typical specimen in wet state directly after preparation (left), specimen of **P30** in dry state after swelling in toluene (middle), specimen of **P0** in dry state after swelling in toluene (right).

that provides additional crosslinking but also polar aprotic ester groups to the polymer scaffold. In contrast, solvent uptake and swelling with nonpolar toluene is high. Both parameters are decreasing with increasing **CLC** content. While **P0** takes up 1148 ± 19 w% toluene upon swelling by 63 ± 2.3 v%, **P40** accommodates only 555 ± 16 w% toluene upon swelling by

30 ± 1.5 v%. A combination of the higher crosslinking degree and a more polar polymeric phase is held responsible for the observed trend (Figure 4a and b). Successively the swollen specimens were dried under ambient conditions until constant mass was observed. In all cases complete drying was found, i.e. within experimental error masses after drying were the same as those measured before swelling. However, samples shrunk to a different degree when compared to the dimensions before immersion into the solvents (Figure 4c). The shrinkage is rather insignificant when water has been accommodated and amounts to 1-3 v%. Less polar solvents lead to higher volume shrinkage of in the range of 2-8 v% (ethanol, *n*-propanol and acetone) but in all cases the original disc shape of the specimens was conserved. In case of the least polar solvent toluene and **P0** the pronounced shrinkage of 221 v% was observed, i.e. the original shape of specimens was lost (Figure 4d). In contrast, **CLC**-bearing foam specimens **P10-P40** recovered their original shape showing low (**P10**, ≈ 9 v%; **P20** ≈ 7 v%) or no (**P30**, ≈ 0 v%) volume shrinkage. **P40** even expanded by on average 3 v%. In all solvent cases the lowest shrinkage upon drying was observed for **P40** featuring the highest **CLC** loading. Specimens of **P10-P40** were again tested for their porosity and their morphology and no significant difference in respect to the values from before swelling could be noted (Figure S7 and S8). This behavior can be regarded as a solvent programmed shape memory effect.^[42] The specimens are programmed during molding, exhibit an omnidirectional swelling in toluene and recover their original shape upon drying or changing the solvent for acetone. The (higher) crosslinking in **P10-P40** is supposed to be responsible for the effect.

2.5. Mechanical Properties

Finally, the mechanical properties of the foams were assessed by tensile testing and results are gathered in Figure 5 (and Table S1). In essence, it became clear that the ductility is decreasing while the stiffness of the samples is increasing with increasing **CLC** content (Figure 5a). The

Young's modulus (reflecting the stiffness) of the polymer foams is steadily increasing from 103 ± 3 MPa for **P0** to 117 ± 3 MPa in **P40** (Figure 5b).

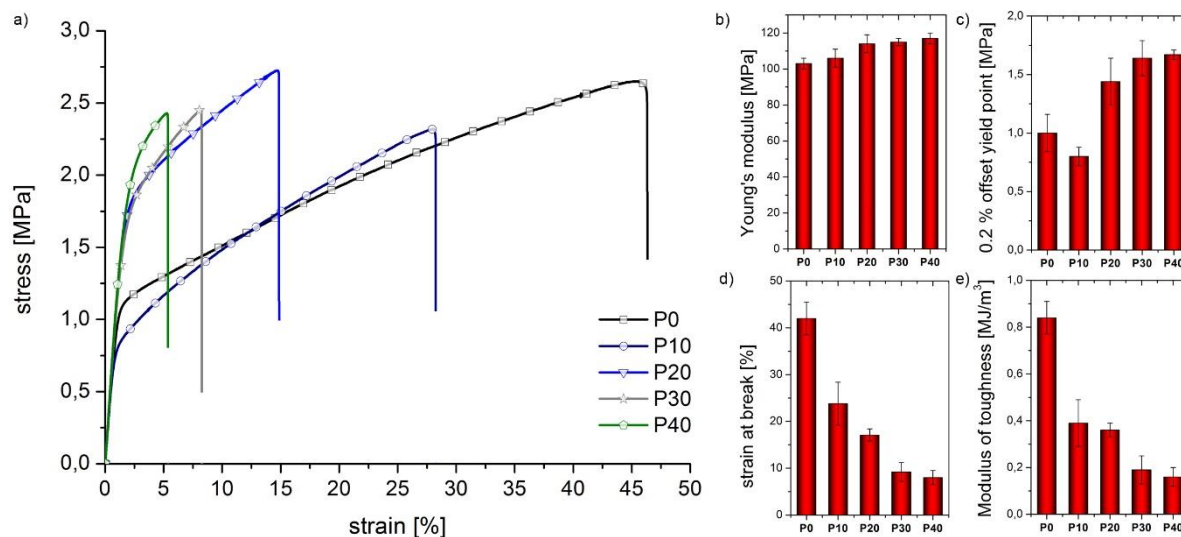


Figure 5. a) stress strain curves for foams **P0-P40**; diagrams of the b) Young's modulus; c) 0.2% offset yield strengths; d) strain at break and e) modulus of toughness of **P0-P40**.

These values are higher than the Young's modulus of carefully extracted **pDCPD** foams prepared with 7 v% Pluronic L121^[19] and approach those of **pDCPD** foams prepared with 3 v% Pluronic L121.^[21] The yield strength (determined at 0.2% offset) is dropping when going from **P0** (1.00 ± 0.16 MPa) to **P10** (0.80 ± 0.08 MPa) but is then again increasing with increasing **CLC** amount reaching 1.67 ± 0.04 MPa in **P40** (Figure 5c). A similar picture is retrieved for the ultimate tensile strength, which is highest in **P20** (2.72 ± 0.24 MPa) and lowest in **P10** (2.18 ± 0.21 MPa) (Table S1). Both parameters are for all samples lower than those published for the two reference foams discussed above.^[19,21] In contrast, a comparatively high strain at break of 42.0 ± 3.5 % could be observed for **P0**. This high strain at break together with the appealing strength of **P0** foams results in a high modulus of toughness of 0.84 ± 0.07 MJ m⁻³. Actually, to the best of our knowledge, this is the highest modulus of toughness ever reported for a HIPE templated polymer foam of 80% porosity. Strain at break and the modulus of toughness are then decreasing with increasing **CLC** amount (Figure 5d and e). It has been

shown that feature sizes (in particular voids sizes) of the foam and the amount of surfactant remaining in the polymer skeleton are decisive factors for mechanical properties of HIPE templated foams.^[21] Herein, above that, the crosslinking density of the polymer skeleton is influenced by the various amounts of **CLC** in the formulation. The mechanical properties of **P0** are different in respect to similar materials published in literature and that can be ascribed above all to the higher Pluronic L121 share remaining in the polymer skeleton. The surfactant is acting as a plasticizer causing a lowering of the offset yield strength and the ultimate strength and an increase of the strain at break. Switching to the formulations containing **CLC** three aspects have to be considered. First and most important, the **CLC** causes additional crosslinking, which results in decreasing ductility and increasing stiffness and strengths with increasing **CLC** loading. Second, the presence of low amounts of **CLC** allows more Pluronic L121 to be accommodated within the polymer phase, explaining the low offset yield strength and the relatively high strain at break in **P10**. Third, higher **CLC** loadings (i.e. denser polymer networks) more and more override the plasticizing effect of the surfactant leading to much stiffer and more brittle materials. These hypotheses are supported by the swelling/deswelling experiments in particular with toluene. As expected, increasing crosslinking in the series **P0-P40** is causing a decrease in toluene uptake and in swelling and is allowing for recovery of the original shape upon drying. Further support comes from the infrared measurements of the samples after extraction and drying. From there it is evident, that the surfactant amount is increasing from **P0** to **P20** and is then again decreasing from **P20** to **P30** and **P40**.

3. Conclusions

In summary, a series of polyHIPEs of 80% porosity using **DCPD** and a crosslinking comonomer **CLC** as the monomers were prepared and their properties in regard of varying **CLC** contents were studied. The maximum **CLC** loading amounted to 40 w% in respect to the overall monomer mass. High internal phase emulsions with higher **CLC** contents were not

stable under the curing conditions. While porosity as well as voids and window sizes hardly change with increasing **CLC** amounts, the crosslinking degree produced from **CLC** is increasing from 1.7 to 5.8 % when going from **P10** to **P40**. This crosslinking degree is distinctly influencing the mechanical properties of the foams, which become stiffer and less ductile upon increasing the **CLC** amount, i.e. upon enhancing the crosslinking degree. The **CLC** crosslinked foams considerably swell in toluene and recover their original shape and porosity upon drying. This feature distinguishes them from polyHIPEs made from dicyclopentadiene only as drying of toluene swollen **P0** comes with severe shrinkage and a loss of porosity. Accordingly, the herewith introduced **DCPD/CLC** polyHIPEs are suitable for applications which demand repeated swelling and drying of the foams. Furthermore, they are perfectly set-up for post-polymerization functionalization reactions, which should be carried out in nonpolar solvents. In addition, the free norbornene groups introduced into the foams impart the porous materials an enhanced reactivity for post-polymerization functionalization reactions.

4. Experimental Section

4.1. Syntheses

4.1.1. Preparation of butane-1,4-diyl-bis(bicyclo[2.2.1]hept-5-ene-2-carboxylate) (**CLC**)

Freshly distilled cyclopentadiene (8.06 g, 0.122 mol, 2.2 eq) was added dropwise to butane-1,4-diyl diacrylate (10.90 g, 0.055 mol, 1.0 eq) under stirring at a temperature of 4°C. The temperature of the reaction mixture was held below 25 °C (cooling was necessary within the first 2 h). After 6 h the reaction progress was monitored via ¹H-NMR spectroscopy and according amounts of cyclopentadiene (1.6 g) were slowly added to the reaction mixture, which was then heated to 40°C under constant agitation and kept there for 6 h. As the sole by-product

DCPD formed which was removed via flash column chromatography using cyclohexane as eluent. The desired product was eluted with Cy/EtOAc (3:1 (v:v)) in pure form. The solvents were distilled off and the residue was dried in vacuum. Yield: 16.72 g (92 %), colorless liquid, exhibiting an *endo:exo* ratio of 4:1. $R_f = 0.64$ (Cy/EtOAc, 3:1 (v:v)); $^1\text{H-NMR}$ (300 Hz, CDCl_3): $\delta = 6.19$ (m, 2H, $\text{HC}=\text{CH}_{\text{endo}}$), 6.12 (m, 1H, $\text{HC}=\text{CH}_{\text{exo}}$), 5.92 (m, 2H, $\text{HC}=\text{CH}_{\text{endo}}$), 4.11 (m, 2H, $\text{CH}_2\text{CH}_2\text{O}_{\text{exo}}$), 4.05 (s, 4H, 8 $\text{CH}_2\text{O}_{\text{endo}}$), 3.20 (s, 2H, nb1_{endo}), 3.03 (s, 0.5H, nb1_{exo}), 2.97-2.91 (m, 4.5H, nb2_{endo} , nb1_{endo} , nb4_{exo}), 2.21, 1.93-1.86 (m, 3H, nb3_{endo} , nb2_{exo} , nb3_{exo}), 1.68 (m, 5H, $\text{CH}_2\text{CH}_2\text{O}_{\text{endo/exo}}$), 1.42-1.28 (m, 7.5H, nb3_{endo} , nb7_{endo} , nb3_{exo} , nb7_{exo}). $^{13}\text{C-NMR}$ (75 Hz, CDCl_3): $\delta = 176.1$ (2C_{exo} , COOCH_2), 174.9 (2C_{endo} , COOCH_2), 138.0 (2C_{exo} , $\text{HC}=\text{CH}$), 137.9 (2C_{endo} , $\text{HC}=\text{CH}$), 135.7 (2C_{exo} , $\text{HC}=\text{CH}$), 132.4 (2C_{endo} , $\text{HC}=\text{CH}$), 63.9 (2C, $\text{CH}_2\text{CH}_2\text{O}$), 63.8 (2C, $\text{CH}_2\text{CH}_2\text{O}$), 49.6, 46.6, 46.3, 45.7, 43.3, 43.1, 42.5, 41.6, 30.3, 29.2, 25.4. Elem. Anal. calcd: C, 72.70; H, 7.93; O, 19.37; found: C, 72.60; H, 8.06; O, 19.42.

4.1.2. Preparation of the foams **P0-P40**

In a 250 mL three-necked round bottom flask a total amount of 10 g of monomers (according to Table 2), 0.7 g of the surfactant Pluronic L-121 (7 wt% in respect to the total mass of monomers) and toluene (100 μL) were added. The reaction mixture was stirred with a mechanical stirrer at 400 rpm while 40 mL of distilled water was added dropwise over a period of 15 min. Stirring of the formed emulsion was carried on for 1 h. Then the initiator **M2** (molar ratio of 1:15000 in respect to both monomers) dissolved in 200 μL of toluene was added to the emulsion under agitation. The resulting pinky mixture was poured into molds, which were closed and cured at 80 °C for 3 h in an oven operated under air. The demolded specimens were submersed in acetone for 15 min and subsequently dried under ambient conditions until constant weight was reached.

Table 2. DCPD, CLC and initiator amounts used

Sample	DCPD [g] ([mmol])	CLC [g] ([mmol])	Initiator M2 [g] ([mmol])
P0	10.0 (75.6)	-	4.8 (0.0050)
P10	9.0 (68.1)	1.0 (3.0)	4.5 (0.0047)
P20	8.0 (60.5)	2.0 (6.1)	4.2 (0.0044)
P30	7.0 (52.9)	3.0 (9.1)	3.9 (0.0041)
P40	6.0 (45.4)	4.0 (12.1)	3.6 (0.0038)

4.2. Characterization

4.2.1. Swelling/deswelling procedure

The specimens for every copolymer composition were prepared according to 4.2.1. The weight and dimensions of dry samples were recorded. Five solvents exhibiting different polarities at room temperature, water (dielectric constant $\epsilon = 80$), ethanol ($\epsilon = 25$), *n*-pentanol ($\epsilon = 15$), acetone ($\epsilon = 21$) and toluene ($\epsilon = 2.4$) were used for swelling/deswelling experiments. The specimens were immersed into the respective solvent for 24 h and following, the dimensions and weight of wet samples were determined. By calculating the volume for the dry and wet samples and setting those values in relation the swelling degree was retrieved. The solvent uptake was determined by measuring out the mass of the wet sample and was used for calculating the solvent uptake in w%. Afterwards, the specimens were dried under ambient conditions until constant mass was obtained. The dimensions of the dry samples were measured and set into relation with the volume before the swelling procedure. For every formulation **P0-P40** at least five specimens were investigated.

Supporting Information

Supporting Information is available as separate file

Acknowledgements: EV thanks the Onassis Foundation for a stipend. The lead-project LP-03 of Graz University of Technology is acknowledged. We thank C. Wappl for elaborating the synthesis of **CLC**, R. Saf for SEM measurements and Umicore for providing initiator **M2**.

References

- [1] T. Zhang, R. A. Sanguramath, S. Israel, M. S. Silverstein, *Macromolecules* **2019**, *52*, 5445.
- [2] M. S. Silverstein, *Polymer* **2017**, *126*, 261.
- [3] K. M. L. Taylor-Pashow, *Solvent Extr. Ion Exch.* **2019**, *37*, 1.
- [4] J. Zhu, L. Wu, Z. Bu, S. Jie, B.-G. Li, *Ind. Eng. Chem. Res.* **2019**, *58*, 4257.
- [5] R. Zowada, R. Foudazi, *ACS Appl. Polym. Mater.* **2019**, *1*, 1006.
- [6] S. Kovačič, N. Drašinac, A. Pintar, E. Žagar, *Langmuir* **2018**, *34*, 10353.
- [7] Z. Wu, W. Hu, T. Huang, P. Lan, K. Tian, F. Xie, L. Li, *J. Mater. Chem. C.* **2018**, *6*, 8839.
- [8] G. Tripodo, G. Marrubini, M. Corti, G. Brusotti, C. Milanese, M. Sorrenti, L. Catenacci, G. Massolini, E. Calleri, *Polym. Chem.* **2018**, *9*, 87.
- [9] M. Corti, E. Calleri, S. Perteghella, A. Ferrara, R. Tamma, C. Milanese, D. Mandracchia, D. Brusotti, M. L. Torre, D. Ribatti, F. Auricchio, G. Massolini, G. Tripodo, *Mater. Sci. Eng. C* **2019**, in press. DOI: 10.1016/j.msec.2019.110060
- [10] M. Whitely, G. Rodriguez-Rivera, C. Waldron, S. Mohiuddin, S. Cereceres, N. Sears, N. Ray, E. Cosgriff-Hernandez, *Acta Biomater.* **2019**, *93*, 169.
- [11] L. Weinstock, R. A. Sanguramath, M. S. Silverstein, *Polym. Chem.* **2019**, *10*, 1498.
- [12] L. Yang, Y. Liu, C. D. M. Filipe, D. Ljubic, Y. Luo, H. Zhu, J. Yan, S. Zhu, *ACS Appl. Mater. Interfaces* **2019**, *11*, 4318.
- [13] F. Du, L. Sun, W. Tan, Z. Wie, H. Nie, Z. Huang, G. Ruan, J. Li, *Anal. Bioanal. Chem.* **2019**, *411*, 2239.
- [14] E. Vakalopoulou, S. M. Borisov, C. Slugovc, *ChemRxiv* **2019**. DOI: 10.26434/chemrxiv.9124730.v2
- [15] H. Deleuze, R. Faivre, V. Herroguéz, *Chem. Commun.* **2002**, 2822.

- [16] K. Benmachou, H. Deleuze, V. Herrogez, *React. Funct. Polym.* **2003**, *55*, 211.
- [17] S. Kovacic, P. Krajnc, C. Slugovc, *Chem. Commun.* **2010**, *46*, 7504.
- [18] S. Kovačič, K. Jeřabek, P. Krajnc, C. Slugovc, *Polym. Chem.* **2012**, *3*, 325.
- [19] S. Kovačič, N. B. Matsko, K. Jeřabek, P. Krajnc, C. Slugovc, *J. Mater. Chem. A* **2013**, *1*, 487.
- [20] E. H. Mert, C. Slugovc, P. Krajnc, *Express Polym. Lett.* **2015**, *9*, 344.
- [21] S. Kovačič, E. Žagar, C. Slugovc, *Polymer* **2019**, *169*, 58.
- [22] N. Trupej, Z. Novak, Ž. Knez, C. Slugovc, S. Kovačič, *J. CO2 Util.* **2017**, *21*, 336.
- [23] A.-C. Knall, S. Kovačič, M. Hollauf, D. P. Reishofer, R. Saf, C. Slugovc, *Chem. Commun.* **2013**, *49*, 7325.
- [24] C. L. McGann, G. C. Daniels, S. L. Giles, R. B. Balow, J. L. Miranda - Zayas, J. G. Lundin, J. H. Wynne, *Macromol. Rapid Commun.* **2018**, *39*, 1800194.
- [25] R. B. Balow, S. L. Giles, C. L. McGann, G. C. Daniels, J. G. Lundin, P. E. Pehrsson, J. H. Wynne, *Ind. Eng. Chem. Res.* **2018**, *57*, 8630.
- [26] S. Kovačič, F. Preishuber-Pflügl, D. Pahovnik, E. Žagar, C. Slugovc, *Chem. Commun.* **2015**, *51*, 7225.
- [27] S. Kovačič, H. Kren, P. Krajnc, S. Koller, C. Slugovc, *Macromol. Rapid Commun.* **2013**, *34*, 581.
- [28] S. Kovačič, N. B. Matsko, G. Ferik, C. Slugovc, *J. Mater. Chem. A* **2013**, *1*, 7971.
- [29] S. Kovačič, A. Anžlovar, B. Erjavec, G. Kapun, N. B. Matsko, M. Zigon, E. Zagar, A. Pintar, C. Slugovc, *ACS Appl. Mater. Interfaces* **2014**, *6*, 19075.
- [30] E. Yüce, E. H. Mert, P. Krajnc, F. N. Parin, N. San, D. Kaya, H. Yildirim, *Macromol. Mater. Eng.* **2017**, *302*, 1700091.
- [31] E. Yüce, P. Krajnc, H. H. Mert, E. H. Mert, *Appl. Polym. Sci.* **2019**, *136*, 46913.

- [32] S. Kovačič, M. Mazaj, M. Jeselnik, D. Pahovnik, E. Žagar, C. Slugovc, N. Zabukovec Logar, *Macromol. Rapid Commun.* **2015**, *36*, 1605.
- [33] M. Mazaj, N. Zabukovec Logar, E. Žagar, S. Kovačič, *J. Mater. Chem. A* **2017**, *5*, 1967.
- [34] M. Scharfegger, B. Fuchsbichler, S. Koller, C. Slugovc, S. Kovacic, (Varta Micro Innovation GmbH, Technische Universität Graz) WO2013178371A1, **2013**.
- [35] S. M. Andler, J. M. Goddard, *J. Agric. Food Chem.* **2018**, *66*, 3619.
- [36] S. Kovačič, F. Preishuber-Pflügl, C. Slugovc, *Macromol. Mater. Eng.* **2014**, *299*, 843.
- [37] A.-C. Knall, C. Slugovc, *Chem. Soc. Rev.* **2013**, *42*, 5131.
- [38] A.-C. Knall, M. Hollauf, C. Slugovc. *Tetrahedron Lett.* **2014**, *55*, 4763.
- [39] C. E. Hoyle, C. N. Bowman, *Angew. Chem. Int. Ed.* **2010**, *49*, 1540.
- [40] C. N. Walker, J. M. Sarapas, V. Kung, A. L. Hall, G. N. Tew, *ACS Macro Lett.* **2014**, *3*, 453.
- [41] A. Leitgeb, J. Wappel, C. A. Urbina-Blanco, S. Strasser, C. Wappl, C. S. J. Cazin, C. Slugovc, *Monatsh. Chem.* **2014**, *145*, 1513.
- [42] D. Chen, X. Xia, T. W. Wong, H. Bai, M. Behl, Q. Zhao, A. Lendlein, T. Xie, *Macromol. Rapid Commun.* **2017**, *38*, 1600746.